Autler-Townes triplet absorption spectroscopy, controllable electromagnetically induced transparency and nonlinear coherence Kerr effect

Bakht A Bacha
Department of Physics, Hazara University, Monsehra, Pakistan

Fazal Ghafoor
*Department of Physics, COMSATS Institute of Information Technology, Islamabad, Pakistan**

Rashid G Nazmitdinov
Laboratory of Theoretical Physics JINR, Moscow Region, Dubna, Russia

arXiv:1401.2098v3 [physics.optics] 1 Feb 2014

A Field Generated Coherence (FGC)' based 3-field cyclically-driven 4-level atomic system, which is an extended version of Λ type schemes, is investigated for Autler-Townes Triplet (ATT) absorption spectroscopy. Two dark lines which appear in the ATT spectrum, are the essence of the generated multiple controllable Electromagnetically Induced Transparency (EIT) windows for a superluminal Gaussian light pulse. We also investigate enhancement in the group advance time for a probe superluminal Gaussian light pulse even with no additional losses while generating nonlinear coherence Kerr effect through an intense monochrmatic laser field. Consequently, the pulse leaves the steep anomalous region of the medium by $38\mu s$ sooner than the pulse when retrieved from the Kerr-free system. A co-linear propagation of the driving fields is suggested to minimize our explored incoherence Doppler broadening effect on the probe pulse. Indeed, the analytically observed undistorted retrieved Gaussian light pulse, which is a necessary and useful requirement for realization of the results in laboratory, is also shown and analyzed explicitly.

I. INTRODUCTION

Generally, when the excited state is coupled with a third level by strong laser field through an allowed electric dipole transition, the excitation signal from a ground level is modified. The excited signal appears as two distinct components, a pattern often termed the Autler-Townes (AT) doublet [1–4].

This phenomenon has been extensively studied in the context of spontaneous emission spectrum [5–11], stimulated absorption [12–16], their population dynamics [17–20], wave mixing [21–25] and in some restricted conditions in context of Electromagnetically Induced Transparency (EIT) [30, 31]. Ideally, in a AT doublet spectrum, a dark line arises due to quantum interference in the probed excitation signal. This dark line which is the essence of EIT, is traced back to the interference effect between alternative transition pathways created by the coupling fields with the internal states of the quantum system. [1–4, 8]. The EIT based schemes in some specific cases of a dispersion regions also result in slowing the group velocity of a subluminal probing pulse. One of the mechanisms to significantly slow-down a propagating pulse in connection with a slow light, is the nonlinear coherence Kerr effect used by Agarwal and Dey [29].

In this paper, a 4-level atomic scheme which is an extended version of Λ type schemes, is investigated for AT triplet absorption spectroscopy. The physical mechanism of this scheme is rigorous, novel and useful. Unlike AT doublet, the excitation signal from the ground level appears as three distinct components in the ATT spectrum caused by the quantum interference effect among the three excitation probability amplitudes of the probed light pulse. Consequently, two dark lines appear in the absorption spectrum. The behavior of the interferences lead to splitting of the single Lorentzian-like absorption line spectrum into three components separated by two dark lines in a way obeying Weisskopf-Wigner theory of a spectral line. Intriguingly, the multiple interference mechanisms provides multiple dispersion regions for an ideal transparency of a weak probe light pulse. However, unlike the AT doublet, this triplet system provides multiple steeped anomalous regions where the probe light pulse gets superluminal. Further, unlike AT doublet, here in the triplet spectroscopy, the role of the Kerr effect on the superluminal probe pulse is contrastingly counterintuitive. Instead to decrease the group velocity, the Kerr effect enhances the group velocity of the probed pulse in the multiple anomalous regions of the dispersion medium. Furthermore, avoiding incoherence Doppler effect in a system is also important from experimental point of views. Therefore, we also analyzed our system for Doppler broadening effect if a gas medium with a hot temperature is considered. Various scenarios of the incoherent Doppler-broadening are also explored. Therefore, a co-linear propagation of the driving fields with low temperature medium is suggested to minimize our explored incoherence effect of the broadening in the system. The combination of the these two processes may further enhance the superluminal group velocity to an ultimate limit for our system.

An EIT based scheme is accompanied with an absorb-

*Electronic address: rishteen@yahoo.com

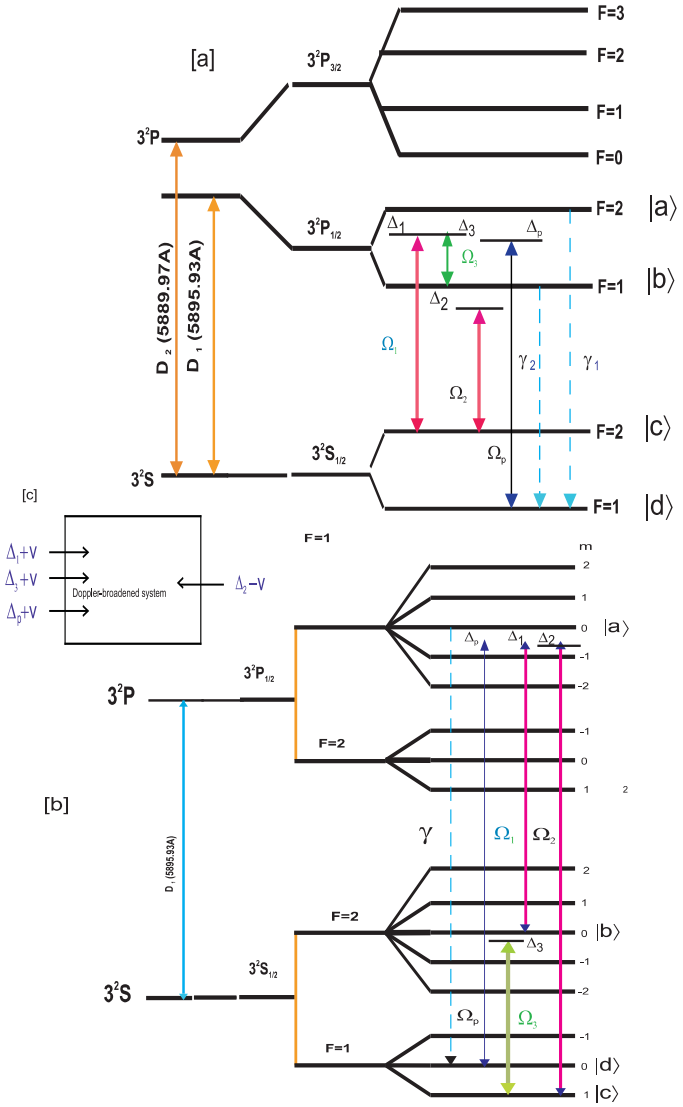

FIG. 1: (a): Schematics of a system based on example of atomic Sodium D1 line. (b): Schematics of the system based on example of hyperfine Sodium D1 line for an ideal AT triplet spectrum [c]: Orientation of driving fields relative atomic motion for both (a) and (b).

tion at dispersion region of a medium more often. The experimental viability of a superluminal light pulse is always conditioned by a relatively less distorted pulse at the output. Here, the development of the coherence in the system via nonlinear Kerr effect increases the negative group index significantly while exhibiting relatively almost no absorption at some anomalous regions of the medium. Consequently, the Gaussian pulse retrieved remains almost undistorted for the Kerr effect even with a significant enhancement in the group velocity. We evaluated analytically the expression for the retrieved Gaussian pulse using transfer function of the medium as a convolution. Evidently, the retrieved Gaussian pulse remains almost undistorted, a remarkably useful characteristics of the system. Therefore, it may be appealing for researchers of the area to demonstrate the phenomenon of the AT triplet absorption spectroscopy, its connection with EIT, superluminality and its enhancement, in laboratory.

II. MODEL AND EQUATION

Consider a 4-level atomic system based on the hyperfine-structured atomic Sodium Na^{23} D1 line ($3S^2_{1/2} \Longleftrightarrow 3P^2_{1/2}$) [see Fig. 1(a)]. Two excited levels of $3^2P_{1/2}$,F=2 i.e., ($|a\rangle$) and $3^2P_{1/2}$,F=1 ($|b\rangle$) of the excited doublet are driven by a microwave field of Rabi-frequency Ω_3. These closely spaced levels are then coupled with the ground state $3^2S_{1/2}$,F=2 ($|c\rangle$) via two coherent optical fields of Rabi frequencies Ω_1 and Ω_2, respectively. The selected excited two closely spaced states decay to second ground state, $3^2S_{1/2}$,F=1 ($|d\rangle$) (allowed transitions) due its coupling with the vacuum field modes. Also a weak probe field is coupled with the ground state $3^2S_{1/2}$,F=1 ($|d\rangle$) and the excited state ($|a\rangle$) with the coupling Rabi frequency Ω_p. Initially, we assume the coupling of the optical fields and the microwave field detuned from their respective atomic transition frequencies. Therefore, the optical fields detunings are chosen as $\Delta_1 = \omega_{ca} - \nu_1$ and $\Delta_2 = \omega_{cb} - \nu_2$ while the detuning of the microwave field from the upper closely spaced levels is $\Delta_3 = \omega_{ba} - \nu_3$. Nevertheless, the probe field detuning is selected as $\Delta_p = \omega_{da} - \nu_p$. The response of the medium due to the interaction of these fields with the atomic system under consideration can be found from the susceptibility of the system. To calculate this susceptibility we evaluate the rate equations while using the following Hamiltonian in the interaction and rotating wave approximation:

$$\begin{aligned} H_I &= -\frac{\hbar}{2}\Omega_3 e^{i\Delta_3 t}e^{i\varphi}\,|a\rangle\langle b| - \frac{\hbar}{2}\Omega_2 e^{i\Delta_2 t}\,|b\rangle\langle c| \\ &\quad -\frac{\hbar}{2}\Omega_1 e^{i\Delta_1 t}\,|a\rangle\langle c| - \frac{\hbar}{2}\Omega_p e^{i\Delta_p t}\,|a\rangle\langle d| + H.c. \end{aligned} \quad (1)$$

To find out the equations of motion we use the following general form of density matrix equation

$$\frac{d\rho}{dt} = -\frac{i}{\hbar}[H_I, \rho] + \Lambda\rho, \quad (2)$$

with $\Lambda\rho$ expressed in the LineBland form for damping part of our system is given as:

$$\Lambda\rho = -\frac{1}{2}\Gamma_{ij}\sum(\sigma^\dagger\sigma\rho + \rho\sigma^\dagger\sigma - 2\sigma\rho\sigma^\dagger),$$

where $\sigma\,(\sigma) = |a\rangle\langle d|(|b\rangle\langle d|)$ and $\sigma^\dagger\,(\sigma^\dagger) = |d\rangle\langle a|(|d\rangle\langle b|)$ are the lowering and raising operators for the two decay transitions of the system, respectively. After straight forward calculation we obtain the three coupled rate equations in the first order as:

$$\begin{aligned} \dot{\rho}_{ad} &= -(i\Delta_p + \frac{1}{2}\gamma_1)\rho_{ad} + \frac{i}{2}\Omega_3 e^{i\varphi}\rho_{bd} \\ &\quad + i\frac{i}{2}\Omega_1\rho_{cd} - \frac{i}{2}\Omega_p(\rho_{aa} - \rho_{dd}), \end{aligned} \quad (3)$$

$$\dot{\rho}_{bd} = -[i(\Delta_p-\Delta_1)+\frac{1}{2}\gamma_2)]\rho_{bd}+\frac{i}{2}\Omega_3^* e^{-i\varphi}\rho_{ad} +\frac{i}{2}\Omega_2\rho_{cd}-\frac{i}{2}\Omega_p\rho_{ba}, \quad (4)$$

$$\dot{\rho}_{cd} = -i(\Delta_p-\Delta_3)\rho_{cd}+\frac{i}{2}\Omega_1^*\rho_{ad} +\frac{i}{2}\Omega_2\rho_{bd}-\frac{i}{2}\Omega_p\rho_{ca}. \quad (5)$$

Next, we consider the atom initially in the ground state $|d\rangle$ i.e., $\rho_{dd}=1$, $\rho_{aa}=0$, $\rho_{ba}=0$, $\rho_{ca}=0$. The above set of equations can be solved for ρ_{ad} using the equation

$$R(t)=\int_{-\infty}^{t} e^{-Q(t-t')}Pdt' = Q^{-1}P, \quad (6)$$

where $R(t)$ and P are column matrices while Q is a 3x3 matrix. The solution is obtained as:

$$\rho_{ad}=-\frac{RA+B\Delta^2+i[A\Delta^2-RB]}{A^2+B^2}\Omega_p, \quad (7)$$

where

$$A = 2\gamma_1\gamma_2(-\Delta_3+\Delta_p)-2[4(\Delta_3-\Delta_p)\Delta_1\Delta_p+\Delta_1\Omega_1^2] +2\Delta_p(4(\Delta_3-\Delta_p)\Delta_p+\Omega_1^2+\Omega_2^2)+2(-\Delta_3+\Delta_p)\Omega_3^2 +2\Omega_1\Omega_2\Omega_3\cos\varphi, \quad (8)$$

$$B = 4\gamma_1(-\Delta_3+\Delta_p)(\Delta_1-\Delta_p)+\gamma_1\Omega_2^2 +\gamma_2[4(\Delta_3-\Delta_p)\Delta_p+\Omega_1^2], \quad (9)$$

and

$$R=4(\Delta_3-\Delta_p)(\Delta_p-\Delta_1)+\Omega_2^2. \quad (10)$$

The susceptibility is a response function of a medium due its interaction with external fields. Here, our atomic medium interacts with multiple coherent fields of different nature. Therefore, the susceptibility of the interacting medium mainly depends on orientation and strength of these fields, the selected atomic medium and the nature of the interacting environment. In this connection, the physical behavior of the system can be evaluated by the relation of the polarization of the medium defined by P=$\epsilon_0\chi E$ and the coherently generated polarization of the probe field define by P=$|\wp_{ad}|^2\rho_{ad}$ (where $\wp_{ad}$ is the dipole matrix element). Now comparing the two polarizations we get the expression for the susceptibility as [61]:

$$\chi=\frac{2N|\wp_{ad}|^2}{\epsilon_0\hbar\Omega_p}\rho_{ad}, \quad (11)$$

where ρ_{ad} is given by Eq. (7). To explore various fact concerned with the dynamical behavior of the probe pulse in the medium we need to evaluate the group index for this system. It is further related with the group velocity v_g via N_g=c/v_g , where c is the speed of light in vacuum. Therefore, the group index is calculated as:

$$N_g=1+2\pi Re[\chi]+2\pi\omega_{ac}Re[\frac{\partial\chi}{\partial\Delta_p}]. \quad (12)$$

Next, we assume the conditions of our proposed system general and also consider Doppler frequency shift if a medium with a hot temperature is selected. Under this consideration the Doppler frequency shift is induced by the atomic velocity v relative to the two coherent optical fields, the microwave field and the probe field. The configuration of the counter propagating driving fields through the atomic medium is shown in the Fig. 1c. The Doppler broadening effect in the medium can be introduced through the detuning parameters. According to our selected orientation of the driving fields we chose $\Delta_1=\Delta_1+kv, \Delta_2=\Delta_2-kv, \Delta_p=\Delta_p+kv$ and $\Delta_3=\Delta_3+kv$ in the susceptibility χ of Eq. (11) [(v is the atomic velocity of the medium). The worked-out susceptibility is then read as:

$$\chi(v)=\frac{2N|\wp_{ad}|^2}{\epsilon_0\hbar}[M(v)], \quad (13)$$

$$M(v)=-\frac{R_1A_1+2\gamma_2(\Delta_3-\Delta_p)B_1+iQ(v)}{A_1^2+B_1^2}, \quad (14)$$

$$Q(v)=[A_1(2\gamma_2(\Delta_3-\Delta_p))-R_1B_1], \quad (15)$$

$$A_1 = 2\gamma_1\gamma_2(-\Delta_3+\Delta_p)+2[-4(\Delta_3-\Delta_p)(\Delta_1+v)(\Delta_p+v) -(\Delta_1+v)\Omega_1^2]+2(\Delta_p+v)[4(\Delta_3-\Delta_p)(\Delta_p+v) +\Omega_1^2+\Omega_2^2]+2(-\Delta_3+\Delta_p)\Omega_3^2+2\Omega_1\Omega_2\Omega_3\cos\varphi, \quad (16)$$

$$B_1 = 4\gamma_1(-\Delta_3+\Delta_p)(\Delta_1-\Delta_p)+\gamma_1\Omega_2^2 +\gamma_2[4(\Delta_3-\Delta_p)(\Delta_p+v)+\Omega_1^2], \quad (17)$$

and

$$R_1=2(\Delta_3-\Delta_p)[2(\Delta_p+v)-2(\Delta_1+v)]+\Omega_2^2. \quad (18)$$

Now, the susceptibility $\chi^{(d)}$ for the Doppler-broadened system which is the average of $\chi(v)$, over the Maxwellian distribution is given by

$$\chi^{(d)}=\frac{2N|\wp_{ad}|^2}{\epsilon_0\hbar V_D\sqrt{\pi}}\int_{-\infty}^{\infty}M(v)e^{-\frac{(kv)^2}{V_D^2}}d(kv) \quad (19)$$

where $V_D=\sqrt{K_BT\omega^2Mc^2}$, is the Doppler width. The corresponding group index can be estimated by

$$N_g^{(d)}=1+2\pi Re[\chi^{(d)}]+2\pi\omega_{ac}Re[\frac{\partial\chi^{(d)}}{\partial\Delta_p}]. \quad (20)$$

The notation we use in the analysis of our mains results of the susceptibility for Doppler-free and Doppler broadened cases are χ and $\chi^{(d)}$ while N_g and $N_g^{(d)}$ are the notations for their group indices.

III. AUTLER-TOWNES TRIPLET ABSORPTION SPECTROSCOPY

In this section we mainly concentrate on the ATT spectroscopy in connection with the absorption and dispersion of a weak probe field propagating through the proposed Sodium atomic medium. Generally, absorption and dispersion mechanisms are very rigorous and complex in nature. Various interesting physical phenomena like gain [26–28], EIT [30, 31], Coherent Population Trapping (CPT) [32], slow [33], fast and backward propagation of light are normally involved [34–40]. Nevertheless, in the present proposal we explore a novel and useful phenomenon of AT triplet absorption spectroscopy and its connection with EIT.

To analyze the dynamical behavior associated with the absorption and dispersion of the probe pulse we quantitatively separate the imaginary χ_{Im} and real χ_{Re} part of the susceptibility χ, respectively. These two parts of the susceptibility are worked-out for the Doppler-free system as:

$$\chi_{Re} = -\frac{2N|\wp_{ad}|^2}{\epsilon_0\hbar}[\frac{RA + 2\gamma_2(\Delta_3 - \Delta_p)B}{A^2 + B^2}], \qquad (21)$$

and

$$\chi_{Im} = -\frac{2N|\wp_{ad}|^2}{\epsilon_0\hbar}[\frac{[A(2\gamma_2(\Delta_3 - \Delta_p)) - RB]}{A^2 + B^2}]. \qquad (22)$$

Furthermore, in the Doppler-free system the spectra of absorption and dispersion are apparently not effectively readable. Nevertheless, the physical behavior of the dynamic may clearly be inspected if we made some reasonable approximation in the system. Further, the introduction of the Doppler effect in the system makes the analytical expressions for the dispersion, absorbtion and their related other physical quantities cumbersome and it is hard to analyzed these parameters conveniently. Nevertheless, these can be estimated from Eq. (19), numerically and graphically. Next, in the following we define some regimes within the spectroscopic parameters for inspection of the results of this system in in association with the Doppler-free system and the Doppler-broadened system simultaneously.

A. $\Omega_3 \gg \Omega_1 = \Omega_2 \approx \gamma_{1,2}$

The behavior of the proposed scheme is complex regarding ATT spectrum and its association with EIT. In this connection quantum interference play an important role. Evidently, if we restrict the intensity of the microwave field coupled with the excited decaying doublet states very large as compared with the intensities of the two optical fields and the decay rates i.e., $\Omega_3 \gg \Omega_1 = \Omega_2 \approx \gamma_{1,2}$, then the effect of quantum interference becomes dominant over the incoherence added by the decay rates to both the Doppler-free and Doppler-broadened

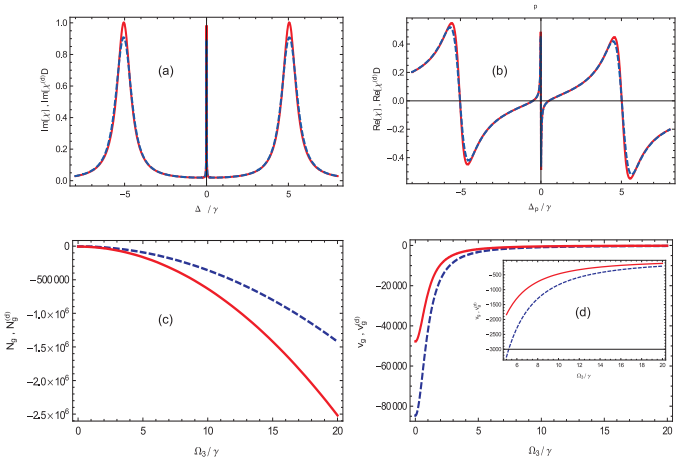

FIG. 2: Absorption and dispersion vs dimensionless probe field detuning, Δ_p/γ, for (a)-(b) when $\gamma = 1MHz$, $\gamma_{1,2} = 1\gamma$, $\omega = 10^3\gamma$, $V_D = 0.5\gamma$, $\Delta_1 = \Delta_3 = 0\gamma$, $\varphi = \pi/2$, $\Omega_{1,2} = 1\gamma$, $\Omega_3 = 10\gamma$ while in (c)-(d) Group index and group velocity vs Ω_3/γ when $\Delta_p = 0\gamma$.

cases. As a result the interference effect generates two dark lines in their absorption spectra and split these into triplets as shown in Fig. 2(a) while their steeped anomalous behavior around the very narrowest absorptions are shown in Fig. 2(b). Nevertheless, the dark lines appear with a reduced absorption and dispersion in the case of the Doppler-broadened system [The red solid (blue dash) line stands for Doppler-free (Doppler broadened)]. Their corresponding group indices and group velocity are also shown in Fig. 2 (c) and Fig. 2(d) where the extremely large enhanced group indices appear for the more steeped anomalous dispersion regions associated the two dark lines of the absorption spectra. Here, it is easy to interpret the physical behavior of the system. Keeping the strength of the microwave field very larger than both the involved decay rates and the strength of the optical fields, the oscillation of the atom between the upper closely spaced doublet becomes very fast as compared with oscillation in between the other states of the atom. Quantitatively, the oscillation between the excited doublet states is as fast the strength the microwave as greater than the optical wave fields. Consequently, the emission probability from the decaying states of the doublet is reduced significantly even then if the two decay rates also become comparable with the strength of the two optical fields [see Fig. 2(a,b)]. Here, the coherence generated by the microwave field becomes dominant over the incoherence decay processes in both the cases. Consequently, quantum interference effect in the absorption and dispersion spectra is generated for both the Doppler-free and Doppler broadened cases. Nevertheless, in the case of Doppler-free medium it is easy to estimate the locations of the dark lines, the locations of the different spectral components and their Full Widths at Halm Maximum (FWHM). Here, the numerator of χ_I appears

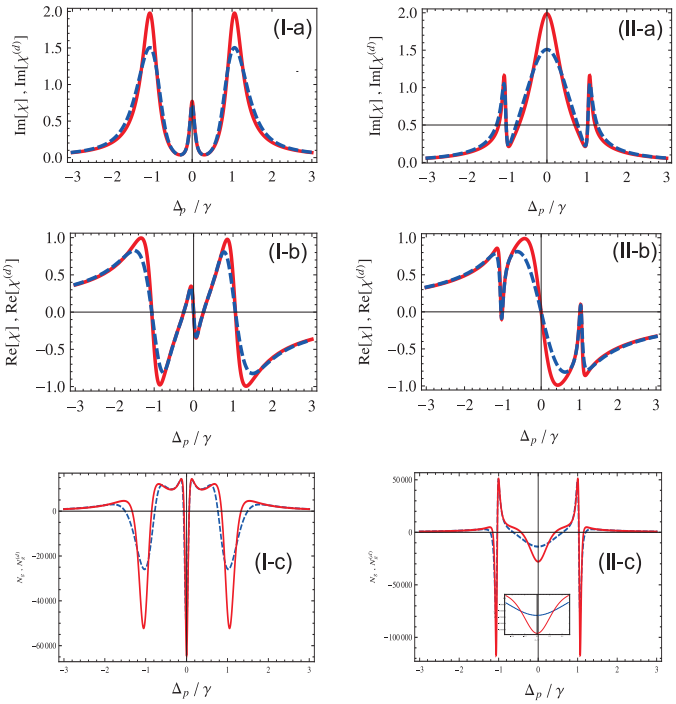

FIG. 3: Absorptions, Dispersions and group index vs dimensionless probe field detuning, Δ_p/γ when $\gamma = 1MHz$, $\gamma_1 = 1\gamma$, $\omega = 10^3\gamma$, $V_D = 0.5\gamma$, $\Delta_1 = \Delta_3 = 0\gamma$, $\varphi = \pi/2$, $\gamma_2 = 0.1\gamma$ and [I]: $\Omega_1 = 2\gamma$, $\Omega_{2,3} = 0.5\gamma$, with similar behavior if Ω_1 and Ω_3 is interchanged. [II]: $\Omega_2 = 2\gamma$, $\Omega_{1,3} = 0.5\gamma$. In this figure, solid line is for Doppler-free case while the dashed blue line is for Doppler-broadened.

as $[\sum_{i=1-3}\Omega_i^2 - 4\Delta_p]\gamma$, if $\gamma = \gamma_1 = \gamma_2$ is considered. In these cases, the absorption spectra vanishes at the two locations i.e., $\Delta_p = \pm\sum_{i=1-3}\Omega_i/2$, which split the single Lorentzian like absorption spectrum into three spectral components. Obviously, the locations of the spectral components appear at $\Delta_p = 0$ and $\Delta_p = \pm\sum_{i=1-3}\Omega_i/2$ while their peak heights can be measured from the Eq. (22). Nevertheless, our numerically estimated values for these physical parameters in the case of Doppler broadening agree with the Doppler-free case. Obviously, the larger Ω_3, the larger is the generated coherence, and consequently, the larger is the negative group index. This behavior becomes more transparent when the group index is plotted against Ω_3/γ and the group velocity as shown in Figs. 2(c) and 2(d), respectively. It can be seen very clearly that the negative group index can be maximized while its corresponding negative group velocity can be minimized, to their ultimate values with increase of the strength of the microwave field. Next, we assume $\gamma_1 \gg \gamma_2$, the numerator of the spectrum of the Doppler-free system becomes as $\Omega_2^2 - 4\Delta_p^2$. Consequently, the spectrum vanishes at the two locations i.e., $\Delta_p = \pm\Omega_2/2$. Nevertheless, keeping γ_1 relatively larger than γ_2 then system behave competitive for coherence-incoherence of the two processes [Fig. 3-I(a,b) and Fig. 3-II(a,b) and compare with Fig. 2(a,b)]. Nevertheless, in case of Doppler broadening the numerically evaluated behavior under similar conditions also agree with the Doppler-free case but with a degraded absorption and dispersion profile. Thus, the dark lines split the single Lorentzian-like absorption spectra into triplets. The plots for their group indices are also shown in Figs. 3-(I-c)) and 3-(II-c). Further, the decay rate from the lower level of an excited pair of hyperfine levels are consider small in its rate by many authors. For example, see the work of Knight and his co-worker on the well famous scheme of quantum beat laser studied in the context of spontaneous emission [50]. The two dark lines appear due to the quantum interference effect among the excitation probability amplitudes. Here, the probe field follows three undistinguished path provided by the three dressed states of the excited real energy level created by the atom-field interaction. The position of the three peaks are located at $\Delta_p = 0$ and $\Delta_p = \pm\sqrt{\sum_{i=1-3}\Omega_i^2 + \gamma_1\gamma_2}$ while the height of the peaks can be estimated from the expression, $\Omega_2^2 - 4\Delta_p^2 G/(A^2+B^2)$, accordingly. Since, the decay process of the system is an incoherent phenomenon, therefore it degrades the interference mechanism significantly. As a result, the dark lines become insignificant with the increase in the decay rates γ_2. The dark lines feature is completely washed out when the decay rate becomes very large. The degradation affect on the interferences mechanism was previously studied extensively in AT doublet absorption, emission and the other triplet based spectra and is consistent with the present study [7, 10]. In principle, the coherence created by the driving fields and the de-coherence phenomenon generated by the decay rates of the excited two hyperfine levels are the two competing phenomena of the system. The larger the coherence of the fields the lesser is the de-coherence of the decay rates and dominant the interference mechanisms is in the system. Next, we notice a drastic change in the widths of the three spectral components with relative strengths of driving fields. The FWHM of the central component decreases with the increase of Ω_1. Nevertheless, it becomes larger for the side peaks correspondingly to obey the Weisskopf-Wigner theory. Furthermore, the peak height also becomes insignificant with larger decay rates as shown in Figs. 3-I(a,b) and 3-II(a,b).

B. $\Omega_{1,2,3} \approx \gamma_{1,2}$

Generally, when the intensities of all the driving fields are kept comparable to the decay rates then the absorption spectrum splits into a triplet but with no quantum interference effect in the system for both the Doppler-free and Doppler-broadened system. Obviously, the triplet is associated with a phenomenon of dynamical Stark triplet splitting. In these cases the quantum coherence developed by the driving fields is not sufficient to overcome incoherence effect added by the decay processes in the

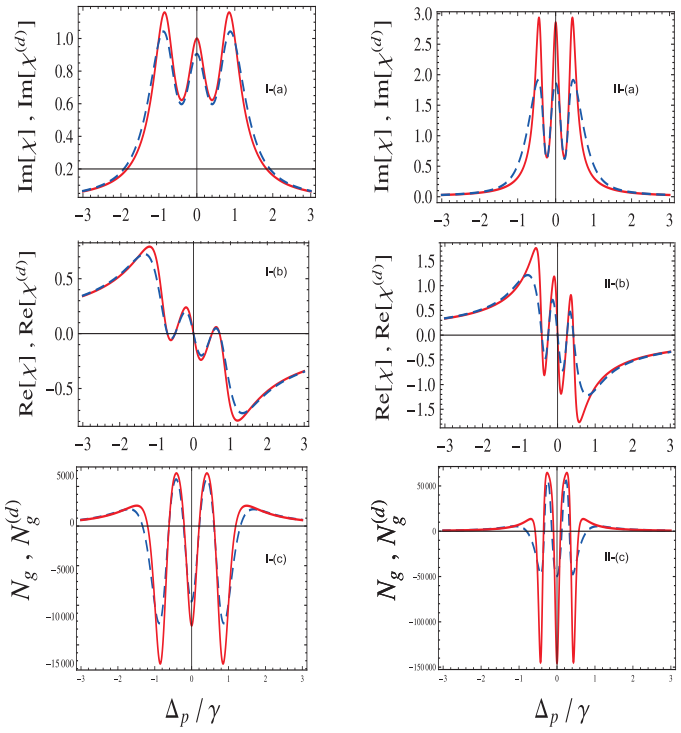

FIG. 4: Absorption dispersion and group index vs dimensionless probe field detuning, Δ_p/γ, when $\gamma = 1MHz$, $\gamma_{1,2} = 1\gamma$, $\omega = 10^3\gamma$, $V_D = 0.5\gamma$, $\Delta_1 = \Delta_3 = 0\gamma$, $\varphi = \pi/2$[I]: $\Omega_{1,2,3} = 1\gamma$, [II]: $\Omega_{1,2,3} = 0.5\gamma$, $\gamma_1 = 0.5\gamma$, $\gamma_2 = 0.2\gamma$.

system. Consequently, the coherence in the absorption process among the three transition probabilities is insignificant and no quantum interference effect is seen in the system [see Figs. 4(I-a) and compare with Fig. 3(I-a)]. Nevertheless, the absorption and dispersion profile for the Doppler-free is more enhanced than the Doppler-broadened case. The corresponding group index follows the dispersion behavior accordingly in Fig. 4(I-c). Nevertheless, it is interesting to note that if in addition to the comparability i.e., $\Omega_{1,2,3} \approx \gamma_{1,2}$, the system decay rates appear smaller, then the behavior of quantum interference also begins to arise as shown in the Figs. 4(II-a) and 4(II-b). The corresponding group indices are also enhanced due to the coherence contributed by the quantum interference in this case as shown in Fig. 4(II-c).

C. $\gamma_2 = 0$

Obviously, the approximation $\gamma_2 = 0$ in the proposed scheme corresponds to an ideal behavior. In principle, the decay rate γ_2 cannot be controlled easily in the system from experimental point of view. Considering the decay γ_2 in its possibly minimum rates, the degradation in the behavior of the quantum interference can be minimized. This is an important aspect of the system which has significant impact on the quantum interference and consequently on the EIT of the probe field. Fortunately, there are some aspects in the system where this ideal behavior of the system can be realized physically.

Consider the Sodium atom now in a weak magnetic field then the ground state and the excited stats of the D1 line appear as Zeeman hyperfine quadruplet [see for example [43]] as shown in Fig. 1(b). Now instead to couple the upper excited hyperfine doublet of the Sodium D1 line as was considered in Fig. 1(a), a ground Zeeman hyperfine doublet is now coupled with the microwave field. Meanwhile, the already microwave-coupled two ground states are coupled with the excited state of the Zeeman quadruplet by two optical fields to form a loop. A weak probe field is then linked with a third ground state and the unique excited decaying state [in the present context] of the quadruplet as shown in the Fig. 1b. This suggested system, we believe to the best of our knowledge, exhibits ideal and experimentally implementable behavior where only one decay mechanism is involved. The absorption and dispersion expressions calculated for this ideal system appear similar to Eq. (21) and Eq. (22) when here the decay rate γ_2 is set to zero. In this way we can easily avoid the decay rate completely from the system in order to avoid the incoherence decay process in the system. It is worthy to mention that all the displayed results in the text associated with the condition $\gamma_2 = 0$, correspond to this ideal and experimentally implementable model.

Next, we extend with the discussion of graphical results for this simple system while considering again the Doppler-free and Doppler-broadened cases. A symmetric absorption and dispersion behavior is obvious in Fig. 5(I-a,b) when the strength of the coherent driving fields is comparable. The FWHM of each of the three spectral components appears $\Gamma/3$ [Γ appears for Einstein decay rate] which obeys Weisskopf-Wigner theory of emission (absorption) of a spectral line. Nevertheless, the spectral profile for the Doppler-broadened case is degraded. Consequently, the group index, group velocity and the advance time of the probe superluminal light pulse decreases with the Doppler broadening effect. Quantitatively, the group index at the region $\Delta_p = 0\gamma$, for Doppler free system are -75397.2, -28273.3 and -452388 when the strength of the coherent fields is gradually increased stepwise. Nevertheless, for the Doppler-broadened system these parameters are estimated as -40000, -24000 and -210000, respectively [see also Fig. 6]. Correspondingly, the time advancement of the probe pulse is also less for Doppler broadened medium as compared with the Doppler-free. The Corresponding group velocity for the Doppler-free system takes $-c/75397.2$, $-c/28273.3$ and $-c/452388$, respectively. Their associated group velocity for the Doppler-broadened medium are measured as $-c/40000$, $-c/40000$ and $-c/210000$, respectively. Further, like the previous cases, this ideal system also exhibits line borrowing and broadening and is consistent with Weisskopf-Wigner theory [see Fig. 5II(a-b) and Fig. 5(III-a,b)]. The corresponding behavior for the negative group indices of the medium for both the Doppler-free and Doppler broadened is shown in Fig. 5(II-a,b) and

Fig. 5(III-a,b), respectively. Further, the FWHM of the central peak increases twice time more than the decrease in the widths of a side peak while increasing the Rabi frequency Ω_3. This phenomenon again agree with Weisskopf-Wigner theory and the sum of the FWHM of the three spectral components is equal to the Einstein natural decay rate. This behavior is similar to the work presented in Ref. [6] but in the context of absorption spectrum. The response of coherence developed by the phase on the spectral profile is also significant and agree with the behavior of a spontaneous emission spectrum reported in Ref. [6] for a 4-level atomic system.

In principle, the Doppler broadening effect is an incoherence phenomenon which degrades the system coherence. As a results it decreases, the superluminal group velocity and consequently, the advance time of the retrieved pulse. Owing to this degradation effect a medium with a cold temperature for co-linear orientation of the driving fields is suggested. We further suggest to prefer a cell in magneto-optical-trap (MOT) [42] over a cavity, where the atomic temperature can be decreased up to few tents μK to minimize the Doppler broadening effect significantly. This will then boost-up the negative group index with a optimum enhancement in the group velocity and advancement pulse time for this system.

IV. CONTROLLABLE BROAD-BAND AND NARROW-BAND EIT WINDOWS

Now, we proceed with analysis of the EIT and its connection with AT triplet absorption spectroscopy. Since, in many conditions two dark lines appear due to quantum interference effect in the spectrum. The corresponding Lorentzian line shape spectrum splits into three components whose sum of the FWHM obey Weisskopf-Wigner theory of a spectral line. These two dark lines are the essence of the EIT and must always be associated as a part of AT absorption spectroscopy under favorably best conditions.

In an ideal case, two dark lines are always there in the spectra when γ_2 is set to zero while keeping the strength of the microwave field and the strengths of the two coherent optical fields same as shown in the Fig. 5(I-a). Interestingly, two transparency windows with equal bandwidth appear for the probe field [see Fig. 5(I-b)]. The widths of these frequency bands are efficiently controlled by the relative strengths of the coherently driving fields. For example, the central peak get narrowed with one of the coherent field. As a results we obtained two narrowest transparency windows around the line center as shown in Fig. 5(II-b). Next, If the relative strength of the other field is increased. The two very narrower transparency windows now appear at displaced location from the central line. As a result we get two extreme narrowed transparency windows at the location displaced from the central line. The results investigated in this system is more elaborative in connection with narrowing and broadening of the transparency windows depending upon the relative strength of the driving fields. In fact, it is the relative strength to make compatible the width of the transparency windows with the FWHM of the weak probe pulse. This compatibility may resolve the issue of pulse distortion in the retrieved pulse a major problem appeared in EIT more often [46]. For example, this behavior is advantage over the behavior of EIT in Refs. [47, 48] in the context of Bose-Einstein condensate, in Refs. [49] in the context of atomic gasious medium and in Refs. [?], in the context of gain medium where no such a controllability over the transparency windows is seen. Furthermore, if the decay rate increases gradually, the dark lines are also eliminated accordingly which is consistent with the Ref. [7] presented in the context of ATT emission spectrum. Ultimately, the transparency of the probe field through the two windows diminishes correspondingly in this specific case [see Fig. 2(b)]. This system is highly sensitive to the coherence developed by the phase of the the coherent field and bring substantial changes in the behavior of the spectrum [5, 51]. As an example, we vary the phase φ to π in Fig. 5(III-a,b) and one of the two sides narrowest transparency window is completely disappeared as shown in Fig. 5(IV-a,b). Consequently, a more broader transparency window with a similar development of incoherence-coherence competing behavior with the decay rates is seen as were discussed in the previous cases. Finally, we conclude that for some specific choices of the strengths of the driving fields we obtain controllable broadband and narrow-band transparency regions for the weak probe field of the system. Interestingly, the controllability of the dark lines and consequently the controllability of the widths of the three spectral components is intriguing and counterintuitive in association with the transparency windows and Weisskopf-Wigner theory for a spectral line. In the earlier many studies, the EIT and its association with the ATT absorption spectroscopy remained unexplored. For example, Sandhya and Sharma presented narrow sharp spectral line within the assumed window of the AT doublet absorption and dispersion specta [52]. In fact, their system lies within the domain of the ATT spectroscopy. The central sharp line in their results may be broadened if an additional optical field is added to form a loop for the three interacting fields. Furthemore, we note that in their scheme two transparency windows appear for the probe field. In Ref. [52] an Y-type atomic system was investigated for a novel mechanism of EIT at the a dispersive region. Nevertheless, their scheme may also be physically interpreted if investigated in the context of ATT absorption spectroscopy associated with the EIT via the Fano-type two dark lines. Controlling EIT within a AT doublet scheme was predicted experimentally via control of a microwave field by Scully and his coworker [53]. Nevertheless, the present scheme provide an efficient control of EIT in both broadband and narrowband windows in the context of a triplet spectrum. Recently, a spontaneous generated coherence based $\bigwedge$ type system linked

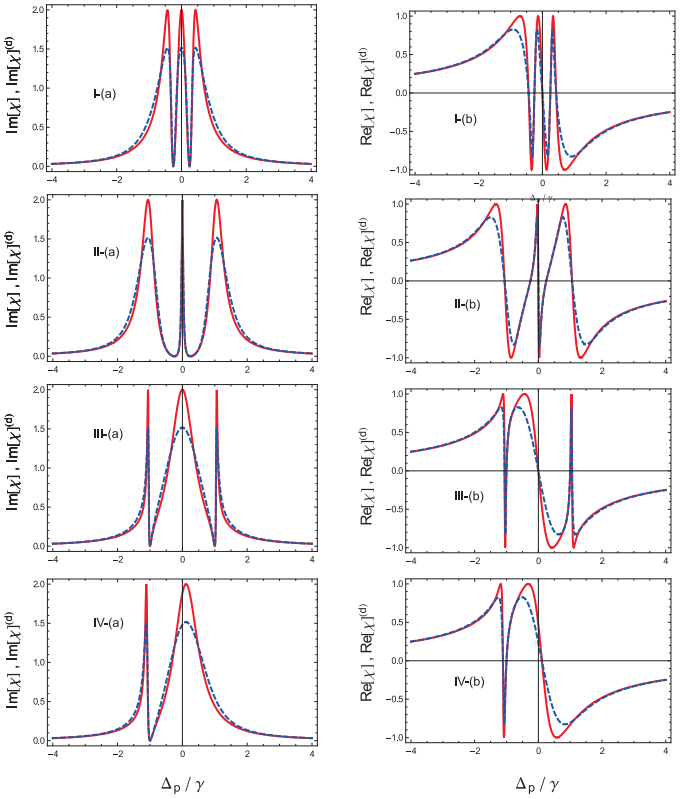

FIG. 5: Absorptions, Dispersions vs dimensionless probe field detuning, Δ_p/γ, when $\gamma = 1MHz$, $\gamma_1 = 1\gamma$, $\omega = 10^3\gamma$,$V_D = 0.5\gamma$, $\Delta_{1,3} = 0\gamma$, $\varphi = \pi/2$, $\gamma_2 = 0\gamma$ [I] $\Omega_{1,2,3} = 0.5\gamma$ [II] $\Omega_1 = 2\gamma$, $\Omega_{2,3} = 0.5\gamma$[III] $\Omega_{1,3} = 0.5\gamma$, $\Omega_2 = 2\gamma$ [IV] $\Omega_{1,3} = 0.5\gamma$, $\Omega_2 = 2\gamma, \varphi = \pi$[V] $\Omega_{1,2} = 0.5\gamma$, $\Omega_3 = 2\gamma$. In the figure, solid line is for Doppler-free case while the dashed blue line is for Doppler-broadened case

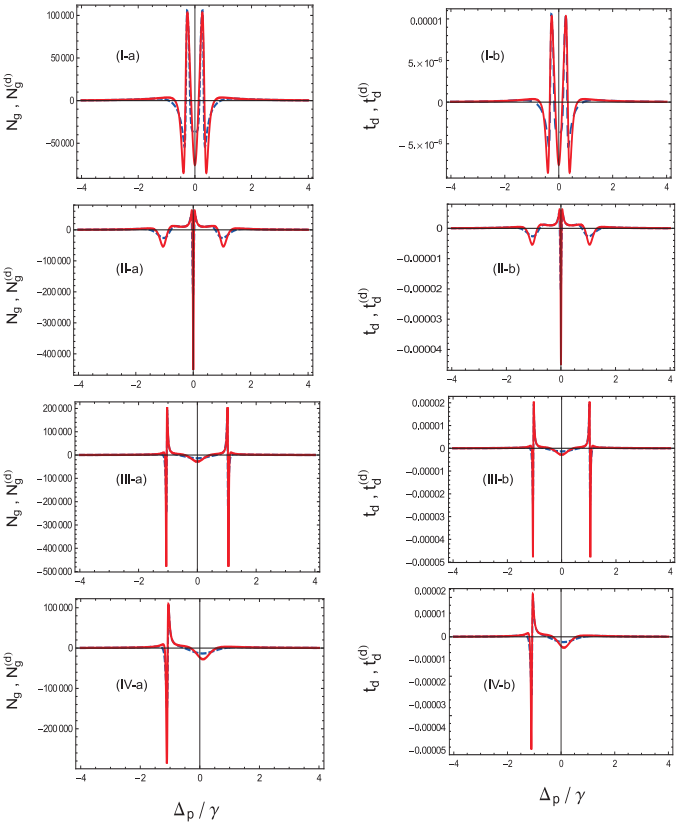

FIG. 6: Group index and group advancement time vs dimensionless probe field detuning, $\frac{\Delta_p}{\gamma}$, when $\gamma = 1MHz$, $\gamma_1 = 1\gamma$, $\omega = 10^3\gamma$, $V_D = 0.5\gamma$, $\Delta_1 = \Delta_3 = 0\gamma$,$\varphi = \pi/2$, $\gamma_2 = 0.0\gamma$ [I]: $\Omega_1 = \Omega_2 = \Omega_3 = 0.5\gamma$, [II]: $\Omega_1 = 2\gamma$, $\Omega_2 = \Omega_3 = 0.5\gamma$, [III]: $\Omega_1 = \Omega_3 = 0.5\gamma$,$\Omega_2 = 2\gamma$. Here, solid line and the dashed blue lines are for the coherence Kerr effect and for the Kerr-free cases while inducing the incoherence Doppler effect in the system.

with dressed states of the Rb^{85} atomic system was investigated both theocratically and experimentally for double transparency windows [56]. Nevertheless, their sophisticated experiment may be best understand in the context of ATT absorption spectroscopy and its connection with with Fano-type quantum interference phenomenon. Furthermore, the spectral narrowing is limited to the central spectral component unlike the present scheme where we can control the width of all the three spectral component obeying Weisskopf-Winger theory for a spectral line. If in their experiment an additional field is couple with the Rb^{85} to form a close loop then the Weisskopf-Weigner theory may be predicted theocratically and experimentally along with narrowing and broadening of all the spectral components. Furthermore, Zhang and his coworker also explores a similar kind of double dark lines feature in the absorbtion spectrum [54] which also requires interpretation in the context of ATT absorption spectroscopy. These kinds of studies exist in literature in details which can also be interpreted very easily from the point of view of ATT absorption spectroscopy [45, 55, 57].

V. SUPERLUMINALITY AND NONLINEAR COHERENCE KERR EFFECT

In this section we investigate the system for enhancing the controllable superluminal and subluminal group velocity using a coherent nonlinear Kerr effect while avoiding the explored incoherence Doppler broadening effect using the traditional experimental techniques. Generally, the nonlinear coherence Kerr effect means a change in the refractive index of a material in response to an applied electric field. It is the electric field intensity dependent nonlinear Kerr effect on the response function of the medium. The corresponding refractive index is proportional to the square or higher order power of the field. Therefore, the change in the refractive index can be measured from $\Delta n_r = \lambda K E_0^{2,4,6,8..}$, where λ is the wavelength and E_0 is the amplitude of the electric field, while K is the Kerr coefficient. Specifically, the Kerr effect in a medium appears due to intense laser light. The susceptibility of the medium may then be related to polarization as $P(\omega) = \epsilon_0\chi(\omega)E(\omega)$, where the electric field

$E(\omega) = E_\omega \cos\omega t$ while E_ω stands for an amplitude of the laser field. If un-important higher order terms are neglected, then the Kerr effect is given by $n_r = n_0 + n_2 I$, where $n_r = \sqrt{1+\chi}$.

One of our goals is also to explore a mechanism in the system for enhancement of superluminality. Here, the available resources are the driving fields itself, and an intense Kerr field may cause significant Kerr effect to the system. The intense Kerr field does not destroy the favorable condition of superluminal pulse as there is no absorption in addition of the propagating probe pulse in the multiple anomalous dispersion regions of the medium.

Our proposed atomic system if also based on nonlinear Kerr effect has various advantages. Some important advantages are: (1) experiment can be conducted in both lower and higher temperature regimes for gaseous, liquid, and solid state mediums; (2) experiment can be conducted if homogenous medium is considered; (3) experiment can also be conducted if inhomogeneous solid state medium is considered, where the density is normally larger and may lead to a larger enhancement in velocity of the superluminaly probe pulse. The unfavorable conditions include: (1) very large optical bandwidth; For a very short and broadband pulses, a deviation from the normal behavior can be observed, (2) very high optical intensity; At extremely high intensity, the Kerr effect becomes saturated and the negative group index may not be increase furthermore.

Now to develop an analytical formalism for the contribution to the system from the nonlinear coherence Kerr effect it can be estimated from the susceptibility χ if expanded in the power series of the Rabi frequency Ω_k [44]. Therefore we write

$$\chi^k = \chi^{(0)} + \frac{1}{2}|\Omega_k|^2 \frac{\partial^2 \chi}{\partial \Omega_k^2}|_{\Omega_k \to 0.} \tag{23}$$

Here, the first term $\chi^{(0)}$ represents the susceptibility when the Kerr field is zero while the second term represents susceptibility contributed by $|\Omega_k|^2$. Obviously, $|\Omega_k|$ is the atom-Kerr-field coupling constant which depends on the Kerr field intensity. The greater is the intensity of the field, the larger is the Kerr effect in the system. To explore the Kerr effect in the system we estimated the susceptibility as

$$\begin{aligned}\chi^k_{Re} &= -\frac{2N|\wp_{ad}|^2}{\epsilon_0\hbar}\Big[\frac{RA_0 + 2\gamma_2(\Delta_3-\Delta_p)B_0}{A_0^2+B_0^2} \\ &+ \frac{\Omega_1^2}{2}\frac{\partial^2}{\partial^2\Omega_1}\frac{RA + 2\gamma_2(\Delta_3-\Delta_p)B}{A^2+B^2}|_{\Omega_1\to 0}\Big] \end{aligned} \tag{24}$$

$$\begin{aligned}\chi^k_{Im} &= -\frac{2N|\wp_{ad}|^2}{\epsilon_0\hbar}\Big[\frac{A_0(2\gamma_2(\Delta_3-\Delta_p)) - RB_0}{A_0^2+B_0^2} \\ &+ \frac{\Omega_1^2}{2}\frac{\partial^2}{\partial^2\Omega_1}\frac{A(2\gamma_2(\Delta_3-\Delta_p)) - RB}{A^2+B^2}|_{\Omega_1\to 0}\Big] \end{aligned} \tag{25}$$

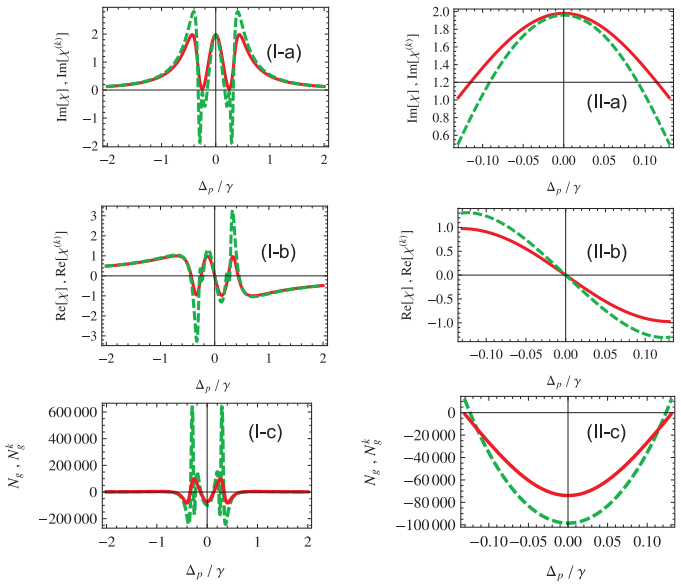

FIG. 7: Absorption dispersion and Group index vs dimensionless probe field detuning, $\frac{\Delta_p}{\gamma}$, when $\gamma = 1MHz$, $\gamma_1 = 1\gamma$, $\omega = 10^3\gamma$, $V_D = 0.5\gamma$, $\Delta_1 = \Delta_3 = 0\gamma$, $\varphi = \pi/2$, $\gamma_2 = 0.0\gamma$, $\Omega_1 = \Omega_2 = \Omega_3 = 0.5\gamma$ [Here, figures II-(a-c) are the insets of figures I-(a-c), respectively]. The solid red lines represent the results for a Kerr-free case while the dashed blue lines show the results for the coherence Kerr effect under same parameters. The absorption profile at the inset shows similar profile for the both the cases. Nevertheless, the dispersion region is more steeper for the coherent Kerr effect than a Kerr-free case. Consequently, the negative group index enhances significantly by the induced nonlinear coherence Kerr effect even with no absorbtion in addition in the system for both the cases.

$$\begin{aligned}A_0 &= -8\Delta_1(\Delta_3-\Delta_p)\Delta_p + 2\gamma_1\gamma_2(\Delta_p-\Delta_3) \\ &+2\Delta_p[4(\Delta_3-\Delta_p)\Delta_p + \Omega_2^2] \\ &+2\Omega_3^2(\Delta_p-\Delta_3) \end{aligned} \tag{26}$$

$$\begin{aligned}B_0 &= 4\gamma_1(\Delta_1-\Delta_p)(\Delta_p-\Delta_3) + \gamma_1\Omega_2^2 \\ &+4\gamma_2(\Delta_3-\Delta_p)\Delta_p \end{aligned} \tag{27}$$

The graphical results of the contribution from the nonlinear coherence Kerr effect are presented Fig. 7. It can be seen that the rate of increase of the negative group indices at some steeped anomalous regions for both the cases are very greater due to the induced Kerr effect even with no absorption in addition at the anomalous dispersion region as compared with a Kerr free system. For example, the absorption close to the region $\Delta_p = 0\gamma$ are same in both Doppler-free and Doppler-broadened system but the dispersion profile for the Kerr effect is more steeped. Consequently, we show analytically a drastic enhancement in the group velocity of the pulse regardless of increase in the absorption probability of the probing Gaussian pulse. Consequently the group index when it is -36950.40 for the Kerr-free system reaches to -49249.10

when there is the nonlinear coherent Kerr effect in the system. Therefore, the pulse advances by $38\mu s$ more than the Kerr-free system. In fact, the applied aspects of superluminality are limited due to severe limitation of the recently developed applications, see for example the references [58, 59] imprecision of temporal cloaking and the reference [60] for imprecision for images measurement. The reason behind these limitations is a small superluminal group velocity of the probe light pulse with a large pulse distortion in the retrieved pulse. The proposed system may be helpful as it qualify for undistorted behavior due its absorption-free behavior with the nonlinear coherence Kerr effect. The undistorted behavior of the retrieved pulse is discussed in the next section.

VI. PULSE DISTORTION

Obviously, the experimental viability of a superluminaly light pulse is conditioned by a relatively less distorted retrieved pulse. Satisfactorily, the analysis of our results reveal smaller absorption rate at anomalous dispersion regions than the relatively more increase rate of the group index even with a Doppler broadening effect in the system. Consequently, we expect, the retrieved Gaussian pulse almost undistorted. The characteristics of shape of the retrieved Gaussian light pulse $S_{out}(\omega)$ by the relation $S_{out}(\omega) = H(\omega)S_{in}(\omega)$, where $H(\omega) = e^{-ik(\omega)L}$ is the transfer function of the medium. The complex wave-number $k(\omega)$ can be expanded via Taylor series in term of group index as:

$$\begin{aligned} k(\omega) &= \frac{N_g^{(0)}\omega}{c} + \frac{1}{2!}(\omega-\omega_0)^2\frac{1}{c}\frac{\partial N_g}{\partial\omega}|_{\omega\longrightarrow\omega_0} \\ &+\frac{1}{3!}(\omega-\omega_0)^3\frac{1}{c}\frac{\partial^2 N_g}{\partial\omega^2}|_{\omega\longrightarrow\omega_0} \\ &+\frac{1}{4!}(\omega-\omega_0)^4\frac{1}{c}\frac{\partial^3 N_g}{\partial\omega^3}|_{\omega\longrightarrow\omega_0}...., \end{aligned} \tag{28}$$

where $N_g^{(0)}$ is the refractive index of the medium at the central frequency ω_0. Next, we consider a Gaussian probe pulse of the form

$$S_{in}(t) = \exp[-t^2/\tau_0^2]\exp[i(\omega_0+\xi)t]$$

propagating through the dispersion region where ξ appears for the upshifted frequency from an empty cavity while the pulse width is represented by τ_0. The Fourier transform of this function is then written by

$$S_{in}(\omega) = \frac{1}{\sqrt{2\pi}}\int_{-\infty}^{\infty} S_{in}(t)e^{i\omega t}dt.$$

The above integral is evaluated analytically and we get

$$S_{in}(\omega) = S_{in}(\omega) = \frac{\tau_0}{\sqrt{2}}\exp[-[(\omega-\omega_0-\xi)\tau_0]^2/4]. \tag{29}$$

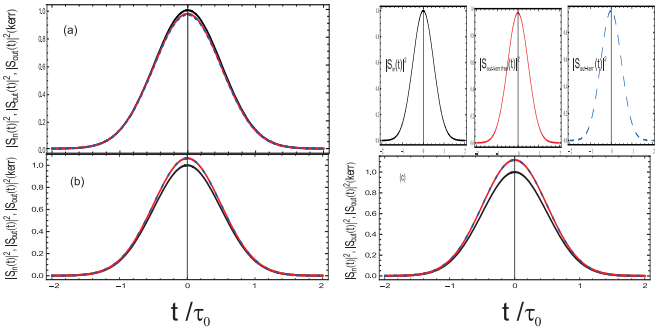

FIG. 8: Input and outputs intensities of the Gaussian pulse vs normalized time. $\gamma_1 = 1\gamma$, $\omega_{ad} = 10^3\gamma$, $\Delta_1 = \Delta_3 = 0\gamma$, $\varphi = \pi/2$, $\gamma_2 = 0.01\gamma$, $\Omega_1 = \Omega_2 = \Omega_3 = 0.5\gamma$, $\tau_0 = 3.5\mu s$, $\omega_0 = 1000\gamma$(a)$\xi = 0\gamma$(b)$\xi = 0.01\gamma$. In the insets(a-c) black represent the input Gaussian pulse. The red lines stand for the retrieved pulse in the case of the Kerr-free medium while the blue represent the retrieved pulse for the Coherence Kerr effect in the system. The distorted pulse shape behavior is shown for different upshifted frequency and an incomparable input pulse width.

Using convolution theorem of the Fourier transforms, the output $S_{out}(t)$ can be written as

$$S_{out}(t) = \frac{1}{\sqrt{2\pi}}\int_{-\infty}^{\infty} S_{int}(\omega)H(\omega)e^{i\omega t}d\omega.$$

Integrating the function analytically we get

$$\begin{aligned} S_{out}(t) &= \frac{\tau_0\sqrt{c}}{\sqrt{2in_1L+c\tau_0^2}}[1-\frac{i(6F_1F_2+F_2^3)n_2L}{48cF_1^3}] \\ &\times\exp[-\frac{\xi^2\tau_0^2}{4}+i(t-\frac{n_0L}{c})\omega_0] \\ &\times\exp[\frac{2ict-2in_0L+c\xi\tau_0^2}{2c}] \\ &\times\exp[\frac{[2ict-2in_0L+c\xi\tau_0^2]^2}{4c(2in_1L+c\tau_0^2)}], \end{aligned} \tag{30}$$

where $F_1 = (2in_1L+c\tau_0^2)/4c$ and $F_2 = (c\xi\tau_0^2 - 2in_1L + 2ict)/2c$.

Furthermore, τ_0 is the input pulse width in time Domain $\Delta_p = \omega_0 - \omega$ while ω_0 (ω) is chosen equal to the atomic frequency (probe field frequency) ω_{ad} (ω_p). Both the group index at the central frequency ω_0 are $n_0 = -36950.40$ and $n_{0k} = -49249.10$. The first and second order derivative of the group index for the Kerr free system are $n_1 = 36.9514$, $n_2 = 5.66953\times10^6$. However, the first and second order derivative of the group index when there is kerr effect in the system are $n_{1k} = 49.25$ and $n_{2k} = 6.17413\times10^6$, respectively. The input pulse width in frequency domain is chosen as $\Delta w = 2\pi/\tau_0$. In Fig. 8, the undistorted characteristics at some anomalous regions and a negligible distorted behavior around the regions with different system parameters is shown explicitly.

VII. SUMMARY

In summary we present a Field Generated Coherence (FGC) based 4-level atomic system driven cyclicly by 3-field linked with an example of hyperfine real Sodium D1 line. The system is investigated for Autler-Townes Triplet (ATT) absorption spectroscopy. The absorption and dispersion spectra of the spectroscopy are then connected with a controllable Electromagnetically Induced Transparency (EIT), enhanced superluminal and enhanced subluminal light pulse propagation. This FGC based system is an extended version of the Λ type schemes of AT doublet and EIT. Here, we explored controllable multiple broad-band and extremely narrow-band windows for transparency of weak probing Gaussian pulse. Two dark lines appear in the spectrum. These dark lines are the essence of the controllable transparency of the probing Gaussian pulse. Intriguingly, we also investigated the system for enhancing the controllable superluminal and subluminal group velocity using coherent nonlinear Kerr effect while avoiding the explored incoherence Doppler broadening effect on the superluminal probe pulse. Further, the rate of increase of negative group index at some steeped anomalous regions are very greater due to the nonlinear coherence induced the Kerr effect even with no losses (absorption)in addition as compared with a Kerr free system. Consequently, we show analytically a drastic enhancement in the group velocity of the pulse but with no losses in addition. In fact, the superluminal probing Gaussian pulse leaves the medium by time of $38\mu s$ sooner than the pulse of the Kerr-free system. Analytical results are presented for pulse distortion measurement for the retrieved Gaussian pulse. Reasonably, due to less lossless characteristics at some anomalous regions of the medium, the retrieved pulse remains almost undistorted. This is a remarkably good condition required for experimental implementation of a superluminal light pulse. Our proposed scheme may also improve precession of the applied aspect of the superluminal light pulse.

Acknowledgment: F G would like to acknowledge the hospitality of the Laboratory of Theocratical Physics during his stay at JINR, Russia (Dubna), where this work was matured.

[1] S. H. Autler and C. H. Townes, Phys. Rev. **100,** 703 (1955).B. Walker, M. Kaluza, B. Sheehy, P. Agostiini, L. F. DiMauro, Phys. Rev. Lett. **75** 633 (1995). P. L. Knight and P. W. Milonni Phys. Rep. **66** 23 (1980): Plastina Francesco and Piperno Francesco, Phys. Lett. A **236** 16 (1997).

[2] U. Fano, Phys. Rev. **124** 1866 (1961); U. Fano and J. W. Cooper, Rev. Mod. Phys. **441** 50 (1968)***.

[3] G. S. Agarwal, Phys. Rev. A **44**, R28 (1991).

[4] G. S. Agarwal *Quantum optics statistical theories of spontaneous emission and their relation to other approaches* edited by G. Höhler *et al.* Springer Tracts in Modern Physics Vol. **70** (1974) (Springer-Verlag, Berlin).

[5] F. Ghafoor, Phys. Rev. A **84** 063849 (2011).

[6] F. Ghafoor F Opt. Commun. **284** 1913 (2011).

[7] F. Ghafoor, S. Qamar, S. Y. Zhu and M. S. Zubairy, Opt. Commun. **273** 464, (2007).

[8] F. Ghafoor, "*Autler-Townes multiplet spectroscopy*". Lasphys **x** xxx (2014)(In press).

[9] D. Agassi Phys. Rev. A **30** 2449 (1984).

[10] S.-Y. Zhu, L. M. Narducci and M. O. Scully Phys. Rev. A **52** 4791 (1995).

[11] E. Paspalakis, C. H. Keitel and P. L. Knight P L, Phys. Rev. A **58** 4868 (1998).

[12] P. Cahuzac and R. Vetter, Phys. Rev. A **14** 270 (1976).

[13] J. E. Bjorkholm and P. F. Liao Opt. Commun. **21** 132 (1077).

[14] H. R. Gray and C. R. Stroud Jr., Opt. Commun. **25** 359 (1978).

[15] C. Delsart, J. C. Keller and V. P. Kaftandjian, J. Phys. **42** 529 (1981).

[16] P. T. H. Fisk, H. A. Bachor and R. J. Sandeman R J, Phys. Rev. A **33**, 2418 (1986).

[17] S.-Y. Zhu and M. O. Scully, Phys. Rev. Lett. **76** 388 (1996).

[18] F. Ghafoor, Lasphys. Lett. **10**, 115002 (2013)

[19] E. M. Macove and C. H. Keitel Phys. Rev. Lett. **91** 123601 (2003).

[20] E. Paspalakis and P. L. Knight Phys. Rev. Lett. **81** 293 (1998).

[21] Y. Zhang, B. Anderson and M. Xiao J. Phys. B **41** 045502 (2008).

[22] Z. Nie, H. Z. P. Li, Y. Yang, Y. Zhang and M. Xiao, Phys. Rev. A **77** 6 (2008).

[23] Y. Du, Y. Zhang, C. Zuo, C. Li, Z. Nie, H. Zheng, M. Shi, R. Wang, J. Song, L. Lu and M. Xiao, Phys. Rev. A **79** 063839 (2009).

[24] C. Li, Y. Zhang, Z. Ni, H. Zheng, C. Zu, Y. Du, J. Song, K. Lu and C. Gan, Opt. Commun. **283** 29182928 (2010).

[25] Y. Zhang, P. Li, H. Zheng, Z. Wang, H. Chen, C. Li, R. Zhang and M. Xiao, Opt. Express **19** 7769 (2011).

[26] L.J. Wang, A. Kuzmich, and A. Dogariu, Nature (London) **406**, 277 (2000).

[27] B. A Bacha, F. Ghafoor, I. Ahmad arXiv:1311.6921, (2013)

[28] B. A Bacha, F. Ghafoor, arXiv:1311.6896, (2013)

[29] T. N. Dey and G. S. Agarwal, Phys. Rev. A **76**, 015802 (2007).

[30] S. E. Harris, J. E. Field and A. Imamoğlu Phys. Rev. Lett **64**, 1107 (1990); K. H. Hahn, D. A. King and S. E. Harris, Phys. Rev. Lett **65**, 2777 (1990); K. J. Boller, A. Imamoğlu and S. E. Harris,Rev. Lett **66**, 2593 (1991); J. E. Field, K. H. Hahn, and S. E. Harris, Phys. Rev. Lett **67**, 3063 (1991); K. Hakuta, L. Mitmet and B. Stoicheff, Phys. Rev. Lett **66**, 596 (1991).

[31] D. Bhattacharyya, B. Ray and P. N. Ghosh, J. Phys. B: At. Mol. Opt. Phys. **40** 4061 (2007);S. Li, X. Yang, X. Cao, C. Xie and H. Wang, J. Phys. B: At. Mol. Opt. Phys. **40** 3211 (2007);M. Fleischhauer, A. Imamoglu, J. P. Marangos, Rev. Mod. Phys. **77** 633 (2005);H. Li, V. A.

Sautenkov, Y. V. Rostovtsev, G. R. Welch, P. R. Hemmer, and M. O. Scully, Phy. Rev. A 80, 023820 (2009);Y. Gu, L. Wang, K. Wang, C. Yang and Q. Gong, J. Phys. B: At. Mol. Opt. Phys. **39** 463 (2006);Shih-Wei Su, Yi-Hsin Chen, Shih-Chuan Gou and I. A. Yu, J. Phys. B: At. Mol. Opt. Phys. **44** 165504 (2011); I. Novikova, R. L. Walsworth and Y. Xiao, Laser Photonics Rev. **6** 333 (2012)

[32] G. Alzetta, A. Gozzini, I. Moi and G. Orriols, Nuovo Cimento, **36B**, 5 (1976); E. Arimondo and G. Orriols, Nuovo Cimento Lett, **17**, 333 (1976); R. M. Whitly and C. R. Stroud, Jr., Phys. Rev. A **14** 1498 (1976); R. Gray, R. M. Whitly and C. R. Stroud. Jr., Opt. Lett. 3, 218 (1978); G. Alzetta, L. Moi, and G. Orriols, Nuovo Cimento, **52B**, 209 (1979); P. M. Radmore and P. L. Knight, Opt. Commun. 42, 411 (1982); S. Swain, J. Phys. B 15, 3405 (1982); G. S. Agarwal and N. Nayak, J. Phys. B 19, 3375 (1986).

[33] Y. Chen, X. G. Wei and B. S. Han, Opt. Express, 17, 1718 (2oo2).

[34] M. S. Bigelow, N. N. Lepeshkin, and R. W. Boyd, Science **301**, 200 (2003).

[35] F. Carreo, O. Caldern, Phys. Rev. A ***71***, 063805 (2005).

[36] A. M. Akulshin, S. Barreiro, Phys. Rev. Lett.**83**, 4277 (1999).

[37] K. Kim, H. S. Moon, C. Lee, K. Kim and J. B. Kim, Phys. Rev. A **68**, 013810 (2003).

[38] H. Kang, L. Wen, Y. Zhu, Phys. Rev. A **68**, 063806 (2003).

[39] F. Xiao, H. Guo, X. Chen, Phys. Lett. A **327**, 15 (2004).

[40] T. J. Kippenberg, S. M. Spillane and K. J. Vahala, Phys. Rev. Lett. **93**, 083904 (2004).

[41] M. Fridman,A. Farsi, Y. Okawachi, Nature, **481**, 62-65 (2012).

[42] E. L. Raab, M. Prentiss, A. Cable, S. Chu and D. E. Pritchard, Phys. Rev. Lett. **59** 2631 (1987).

[43] F. Ghafoor, "*Autler-Townes multiplet spectroscopy*". Lasphys **x** xxx (In revision).

[44] G. S. Agarwal and T. N. Dey, Phys Rev. A **68**, 063816 (2003).

[45] S. N. Sandhya and K. K. Sharma Phys. Rev. A **55** 2631 (1997).

[46] I. Novkova, R. L. Walsworth and Y. Xiao, Laser Photonics Rev. 6, 333 (2012)

[47] J. O. Weatherall and C. P. Search, Phys. Rev. A **78** 013830 (2008).

[48] J. O. Weatherall, C. P. Search and M. Jskelinen Phys. Rev. A **78** 053802 (2008).

[49] Y. Gu, L. Wang, K. Wang, C. Yang and Q. Gong, J. Phys. B: At. Mol. Opt. Phys. 39, 463 (2006); C. L. Wang, A. J. Li, X. Y. Zhou, Z. H. Kang, J. Yung and J. Y. Gao, Opt. Lett. 33, 687 (2008).

[50] E. Paspalakis, C, H. Keitel and P. L. Kinght, Phys. Rev. A **58** 4868 (1998).

[51] F. Ghafoor, S. Y. Zhu and M. S. Zubairy, Phys. Rev. A **62**, 13811 (2000).

[52] B. K. Dutta and P. K. Mahapatra, J. Phys. B: At. Mol. Opt. Phys. **41** 055501 (2008).

[53] H. Li, V. A. Sautenkov, Y. V. Rostovtsev, G. R. Welch, P. R. Hemmer, and M. O. Scully, 80, 023820 (2009).

[54] J. Q. Shen and P. Zhang, Opt. Express **15**, 6484 (2011).

[55] S. Li, X. Yang, X. Cao, C. Xie and H. Wang, J. Phys. B: At. Mol. Opt. Phys. **40** 3211 (2007).

[56] C, L. Wang, A. J. Li, X. Y. Zhou, Z. H. Kang, J. Yun, and J. Y. Gao, Opt. Lett. **33** 687 (2008).

[57] D. Wang and Y. Zheng, Phys. Rev. A **83**, 013810 (2011).

[58] New and Views, R. B. Boyd, Z. Shi, "Macmillan publisher limited", Optical Physics, p 36 (2012).

[59] M. Fridman,A. Farsi, Y. Okawachi, Nature, **481**, 62-65 (2012).

[60] R. T. Glasser, U. Vogl, P. D. Lett, Optics Express**20**, 13702 (2012).

[61] M. O Scully, M.S. Zubairy "*Quantum Optics*", Cambridge University Press, 2000 Cambridge.